JOURNAL OF CATALYSIS 72, 95–110 (1981)

Iron Alloy Fischer–Tropsch Catalysts

III. Conversion Dependence of Selectivity and Water–Gas Shift

J. A. AMELSE,[1] L. H. SCHWARTZ,[2] AND J. B. BUTT[3]

Iptatieff Laboratory, Northwestern University, Evanston, Illinois 60201

Received February 27, 1981; revised June 22, 1981

The performance of several silica-supported iron bimetallic and potassium-promoted iron catalysts has been investigated for the conversion of carbon monoxide to hydrocarbons. The systems studied were Fe–Ni, Fe–Co, Fe–Cu, Fe–K, and the pure metals of Fe, Ni, and Co. Alloy formation and catalyst carburization were characterized using Mössbauer effect spectroscopy. Specific reaction rates, measured in a differential flow reactor at atmospheric pressure, were based on the amount of hydrogen chemisorbed during a novel chemisorption experiment involving flow desorption from catalysts cooled in H_2. When used as synthesis catalysts, the Fe, Fe–K, and Fe–Cu catalysts carburized completely. Alloying Co with Fe suppresses carbide formation. The pure Ni and Co catalysts do not carburize in the reaction mixture although they do carburize in pure CO. The iron–nickel catalysts carburize rapidly but incompletely, with preferential carburization of the bcc phase. Over the 1–6% conversion range studied, Ni, Co, and Fe–Ni showed no turnover frequency sensitivity for CH_4 formation, while Fe, Fe–K, Fe–Cu, and Fe–Co were strongly inhibited, with turnover frequency decreasing by a factor of 2 or more with increasing conversion. The ratio of CO_2/H_2O, used as a measure of water–gas shift activity, was also determined as a function of conversion for the catalysts studied. It was found that the catalysts which are good water–gas shift catalysts are also the ones inhibited during the synthesis. These observations are discussed in terms of a model based on product inhibition by water formation. The olefin/paraffin ratio and its dependence on conversion are reported for all catalysts studied. Synergism is observed upon alloying Fe with Co. The Fe–Co catalyst produced the highest olefin content, has the highest water–gas shift activity, and it also has excellent ability to incorporate olefins into growing chains.

INTRODUCTION

One disadvantage of indirect liquefaction of coal via Fischer–Tropsch catalysis in comparison with direct processes is a net conversion of hydrogen to water. Unless this can be reutilized in the primary gasification step there will be net loss of hydrogen. For example, the olefin-forming reaction

$$2nH_2 + nCO \rightarrow C_nH_{2n} + nH_2O \quad (1)$$

yields 1 mole of water for every mole of carbon entering a hydrocarbon chain. The usage ratio of CO to H during the Fischer–Tropsch synthesis is determined to some extent by the length of the hydrocarbon chains and the degree of saturation. However, since water is the initial oxygen-containing product (*1*), a dominant factor contributing to this ratio is the secondary water–gas shift reaction:

$$H_2O + CO \rightleftarrows CO_2 + H_2. \quad (2)$$

Here, for every mole of water that is not shifted to CO_2, 1 more mole of H_2 is consumed. Hence, a high water–gas shift activity is a desirable feature of a Fischer–Tropsch catalyst.

Secondary reactions are important not only in determining the CO-to-H_2 usage ratio, but also in determining the hydrocarbon product distribution. α-Olefins constitute a major fraction of the initial

[1] Present address: Bell Laboratories, Murray Hill, N.J. 07940.

[2] Department of Materials Science and Engineering and Materials Research Center.

[3] Department of Chemical Engineering; to whom correspondence should be addressed.

0021-9517/81/110095-16$02.00/0

hydrocarbon product and it has been found that olefins may undergo a number of secondary reactions that include hydrogenation, incorporation into growing hydrocarbon chains, and initiation of new chains (*1–5*).

The catalysts used in the present investigation include silica-supported iron and iron bimetallics (Fe–Ni and Fe–Co), as well as potassium- and copper-promoted iron. Iron, by itself, shows relatively high selectivity to olefins and high hydrocarbons, and alkali metals have long been known to be promoters. Dry *et al.* (*6*) observed that potassium promotion increases the heat of chemisorption of CO on reduced iron catalysts and they postulated that promotion occurs by donation of electrons from potassium to iron that in turn increases the donation of electrons from iron to the antibonding orbital of CO upon its adsorption.

Vannice and Garten (*7*) extended these arguments to supported Fe–Pt bimetallic catalysts. Pt should withdraw electrons from iron in the alloy, and hence, one would expect a decrease in rate. Electron withdrawal was confirmed by Mössbauer spectroscopy, and the specific rate over the alloy was indeed lower. However, one must look beyond the metallic state to the state of the catalyst in the presence of the reactants. Iron and potassium-promoted iron form carbides in the presence of the reactant gas (*1*). It may be true that potassium also donates electrons to the carbide. However, in the Fe–Pt system, alloy formation would probably suppress carburization of the catalyst (*8*) and the working Fe–Pt catalysts would then be drastically different from a pure iron catalyst. The alloying agents of this study, Co and Ni, have only small effects on the electronic structure of iron in the alloy, although both are expected to render the iron carbide less stable, with cobalt having a larger effect (*8*).

The extent to which H_2O is shifted to CO_2, and the extent to which olefins are hydrogenated or incorporated into longer chains may be dependent on conversion. Yet, while selectivity data are widely available for many Fischer–Tropsch catalysts, the conversion dependence of selectivity is seldom reported. The present study focuses on the conversion dependence of the secondary reactions at low conversion (1–6% conversion of CO to hydrocarbons up to C_5).

EXPERIMENTAL

1. Catalyst Preparation

The catalysts were prepared by impregnation of 80- to 100-mesh Davison 62 silica gel (average pore diameter of 160 Å) to incipient wetness with the appropriate aqueous solutions of the nitrate salts (potassium was added as a carbonate). Either simultaneous or sequential impregnation was used for the bimetallic and promoted samples as indicated in Table 1 in which compositions of the catalysts studied are listed. After drying at 125°C overnight the samples were calcined in air at 200°C for 2 hr and then at 450°C for 4 hr. Details of the catalysts preparation may be found in Ref. (*9*).

2. Mössbauer Spectroscopy

Details of the spectrometer and data handling are provided elsewhere (*9*). The spectra of this study were obtained from materials which had been treated in the reactor during a normal rate experiment, and then passivated in air. Spectra were recorded at room temperature.

3. Rate Experiments

Rate data were obtained using a tubular ¼-in. o.d. Pyrex reactor. Catalysts were reduced in H_2 at 425°C for 24 hr, then cooled in H_2 to the reaction temperature of 250°C. The reactants were obtained from Airco Industrial Gases as a mixture of 25.9% CO (99.3% min purity) in H_2 (99.999% min pu-

TABLE 1

Catalyst Code, Metal Loading, and H_2 Uptake from Flow Chemisorption

Code	Metal loading (wt%)	Mole ratio Fe : M	H_2 uptake (μmole/g)
Fe-1	4.94		17.8 ± 0.9
Fe-2	9.33		24.7 ± 1.7
Ni-1	4.58		22.6 ± 1.3
Co-1	4.61		23.1 ± 0.5
Fe–Ni-1[a]	3.41 (Fe) 0.83 (Ni)	4.32	13.7 ± 1.7
Fe–Ni-2[a]	2.25 (Fe) 2.37 (Ni)	1.00	17.5 ± 0.7
Fe–Co-1[a]	3.85 (Fe) 1.02 (Co)	3.98	22.7 ± 0.9
Fe–K-1[b]	4.94 (Fe) 0.065 (K)	54	13.7 ± 1.7
Fe–K-2[a]	9.96 (Fe) 0.121 (K)	57	17.5 ± 0.7
Fe–Cu-1[a]	3.6 (Fe) 1.1 (Cu)	3.41	10.6 ± 0.7

[a] Co-impregnation.
[b] Sequential impregnation of calcined Fe-1.

rity), in an aluminum cylinder to reduce carbonyl formation. However, some carbonyls remained and these were removed by a trap of Linde 5A sieve in a dry ice/acetone bath. Successful carbonyl removal was indicated by the lack of an iron "mirror" on the glass reactor. Final oxygen removal was provided by a MnO_2/SiO_2 trap prereduced in flowing H_2. This trap reportedly removes oxygen to less than 1 ppb (*10, 11*), and serves as its own indicator, turning from a blue–green in the reduced state to black as it oxidizes. The reactant mixture contained 0.00064 ± 0.00002 mole fraction of CH_4. Blanks were run every day, and the impurity CH_4 subtracted from the data. Details of the chromatographic separation of the product are provided by Amelse (*9*). All turnover frequencies are based on a surface area measurement determined from the amount of hydrogen chemisorbed during the flow-desorption experiment described in the next section.

4. Hydrogen Chemisorption

Hydrogen chemisorption techniques offer a convenient way of measuring the number of exposed metal atoms directly, however, the stoichiometry must be known. Two opposing factors, thermodynamics and kinetics, make this difficult for some metals such as iron. At constant pressure, higher temperatures lead to lower coverages since adsorption is exothermic; but at low temperatures, where high coverages are favored, adsorption may be too slow since it is an activated process. Hence, maxima are observed in the adsorption isobars if more than one form of adsorption exists.

Hydrogen chemisorption has traditionally been performed in the static mode; however, flow chemisorption techniques have recently been gaining acceptance. Thorough studies have been reported by Freel (*12*) and Sashital *et al.* (*13*).

In performing a flow chemisorption experiment, a reference temperature is chosen. The catalyst is then brought to this temperature by cooling from the reduction temperature (or some other temperature) in either hydrogen or an inert carrier. Traditionally, one chooses the reference temperature to be the temperature that corresponds to the maximum on the isobar. Iron, for example, exhibits an activated form of adsorption with a maximum in the volume adsorbed at about 100°C (*14*). It may be argued that it is not necessary to choose 100°C as a reference temperature for iron if the catalyst is cooled in hydrogen. Upon cooling in hydrogen, the catalyst reaches the temperature where the equilibrium coverage is at its maximum. Upon further cooling, the hydrogen will remain on the surface since desorption is an activated process. Hence, one need not know the optimum temperature, as long as it is bracketed by

the temperature from which the catalyst is cooled in hydrogen and the reference temperature.

In this work the catalyst was reduced in H_2 for 24 hr at 425°C, and then cooled in H_2 to 0°C, the reference temperature, by removing the oven and letting the reactor tube cool in air for 5 min before immersion in an ice bath for 20 min. The reactor was then purged with an argon carrier (O_2 less than 1 ppb) at 0°C, then heated to 425°C for 15 min. A valve was then switched which allowed the desorption pulse to pass to the detector. The detector response was calibrated after each experiment by injecting several pulses of a known amount of H_2 through the reactor which was still at 425°C. A silica blank showed an uptake of 1.5 ± 0.5 μmole H_2/g. This amount has been subtracted before presentation of the data.

The hydrogen uptakes are presented in Table 1 for the catalysts used in this study. These are in general agreement with preliminary efforts to characterize the exposed surface area by physical means (*9*) (X-ray diffraction lineshape analysis and transmission electron microscopy), but the most convincing justification for the use of this technique is agreement of specific activity for catalysts in this study with data in the literature for very similar catalysts. Vannice (*15*) reports methane turnover frequency in which surface area was based on H_2 uptake measured in a classic static apparatus. The results here agree within about 50% for Ni and Co. Unfortunately, the activity of the iron catalysts is strongly conversion dependent, so no comparison could be made to Vannice's data for Fe, for which no conversion was reported.

Since the chemisorption technique is successful for the single-component catalysts, the turnover frequencies for the bimetallic catalysts have also been based on the H_2 uptake measured by this technique. In calculating turnover frequencies, a correction for the extent of reduction has been made based on the thermogravimetric data of Arcuri (*10*), in which the fraction unreduced is taken to be inactive in reaction.

RESULTS AND DISCUSSION

1. Characterization of the Used Catalysts by Mössbauer Spectroscopy

Only data relevant to the extent or suppression of carburization will be presented here. A more detailed Mössbauer effect characterization of all iron-containing catalysts after calcination, reduction, and use in catalyzing the synthesis reactions is provided elsewhere (*9*).

Iron, Fe–K, and Fe–Cu catalysts carburized completely upon exposure to the reactants at 250°C. Potassium and copper had no detectable effect on the extent of carburization or the structure of the carbide; however, Ni and Co had a pronounced effect. Spectra of catalysts Fe–Co-1, Fe–Ni-1, and Fe–Ni-2 are shown in Figs. 1a–c, respectively, with selected fitting parameters summarized in Table 2. Alloying Co with Fe completely suppressed carburization. The Mössbauer spectrum is essentially the same as that recorded after a 24-hr reduction of Fe–Co-1, while the broadening of the peaks indicates that an inhomogeneous Fe–Co bcc alloy is formed (*16*).

Carburization experiments for Fe–Ni-1 and Fe–Ni-2 in a microbalance (*10, 16, 17*) indicate that, although these catalysts carburize incompletely, they carburize rapidly. Mössbauer spectra recorded after 90 min of carburization are essentially the same as those after 3 hr, suggesting that these catalysts reach a steady-state carbide content. The parameters for Fe–Ni-1 with steady-state carbide content indicate that a bcc (iron-rich) alloy remains. Furthermore, a spectrum of this material recorded at liquid N_2 temperature indicates that there is a peak for fcc alloy buried in the central portion of the room-temperature spectrum.

It appears that no Mössbauer data exist in the literature for carefully characterized mixed Fe–Ni carbides. The present data

indicate that the hyperfine fields of the carbide positions have been reduced substantially compared to the value of 174 ± 1 kOe observed for pure iron carbide formed from Fe-1. This suggests that a mixed Fe–Ni carbide has been formed. Such carbides have been observed in meteors (*18*).

The spectrum for Fe–Ni-2 could not be modeled by a computer fit. However, visual inspection of Fig. 1c indicates that material is incompletely carburized, with both magnetically split bcc and fcc phases observed. Comparison of this spectrum to that of Fe–Ni-2 reduced 24 hr indicates that the iron-rich bcc phase preferentially carburizes.

Raupp and Delgass (*19*) have also studied

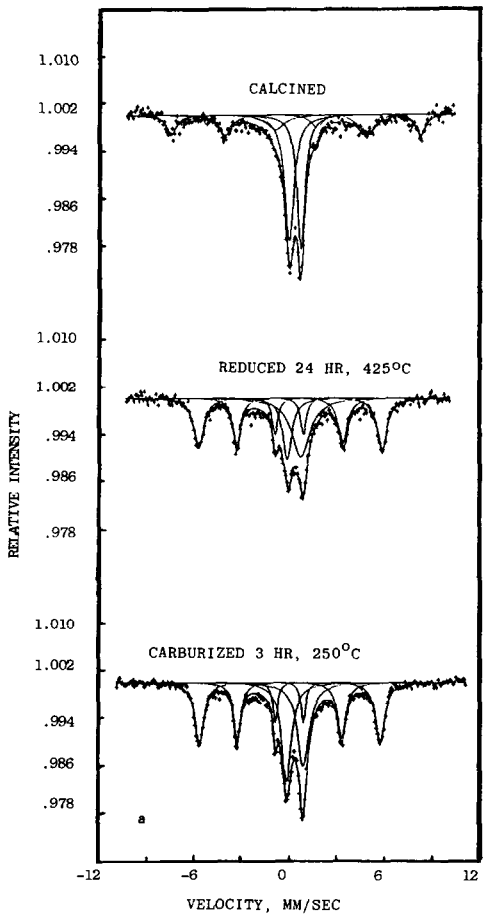

FIG. 1a. Room-temperature Mössbauer spectra of Fe–Co-1.

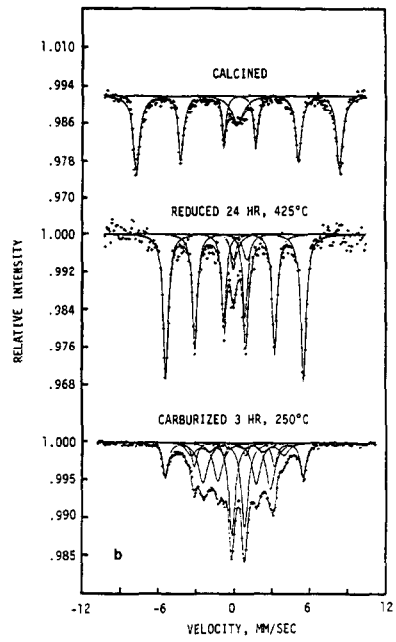

FIG. 1b. Room-temperature Mössbauer spectra of Fe–Ni-1.

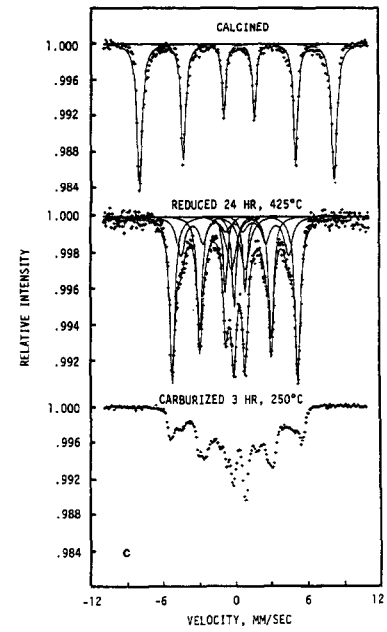

FIG. 1c. Room-temperature Mössbauer spectra of Fe–Ni-2.

TABLE 2

Mössbauer Parameters for Fe–Ni and Fe–Co Alloys

Sample	Compound	I.S.[a] (mm/sec)	Q.S.[b] (mm/sec)	H (kOe)	Area fraction
Fe–Co-1 (Fig. 1a)	(1) bcc Fe–Co alloy	0.02 ± 0.03	−0.03 ± 0.03	354 ± 3	0.56
	(2) Fe^{3+} "oxide"	0.36	1.02		0.44
Fe–Ni-1 (Fig. 1b)	(1) bcc Fe–Ni alloy	0.02[c]	0[c]	338	0.22
	(2) Fe_I carbide	0.22	0.05	162	Fe_I/Fe_{II} = 3.44
	(3) Fe_{II} carbide	0.19	−0.29[c]	227	

[a] Isomer shift with respect to iron metal.
[b] $(V_2 - V_1) + (V_5 - V_6)$ or the distance between a quadrupole doublet.
[c] Constrained to this value.

silica-supported Fe–Ni alloys. They report no carburization of a 1 : 1 Fe–Ni catalyst, which is comparable in composition to Fe–Ni-2; however, their particles were single phase and considerably smaller than those involved here.

2. Rate Data

The term "percentage total conversion of CO to Hc" refers to the conversion of CO to hydrocarbons up to C_5. This quantity does not include CO consumed in forming CO_2. All rate data were obtained at 250°C except data used in calculating activation energies, where the temperature range was 230–280°C, or 240–280°C for the less active catalysts. The steady-state data refer to a time frame of about 40–200 min after the start of the reaction. Samples were injected to the chromatograph about every 30 min. The data represent 4 or 5 days of runs, with fresh catalyst used for every run. In general the catalysts were quite stable; the error bars on the rate data include the contribution of deactivation. In the conversion-dependent experiments, the sequence in which the experiments were run was not monotonic with conversion.

2.1. Conversion dependence of reaction rates. The methane turnover frequency, N_{CH_4}, was found to be independent of conversion for catalysts Ni-1, Co-1, Fe–Ni-1, and Fe–Ni-2 in the range from 1 to 6%. On the other hand, catalysts such as Fe-1 and Fe-2 show quite different behavior, as seen in Fig. 2. Also illustrated is that within error, these two show the same specific rate. This lends further credibility to the reliability of the chemisorption technique, since one would not expect to observe structure sensitivity for these relatively large particles.

Decrease in N_{CH_4} with conversion could, however, also be explained in terms of an

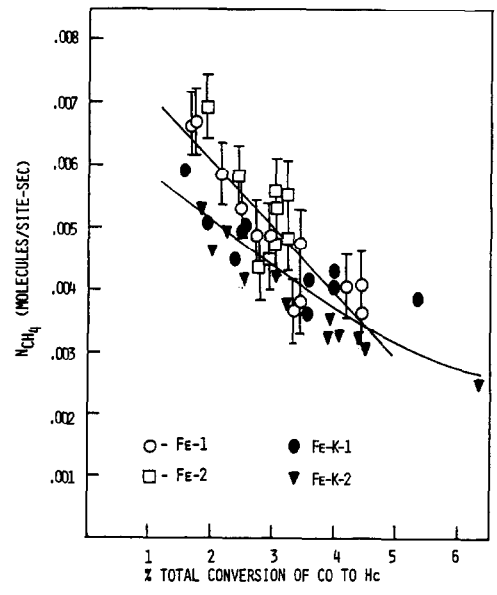

FIG. 2. Conversion dependence of N_{CH_4} for Fe-1, Fe-2, Fe–K-1, and Fe–K-2. Error bars have been omitted from the Fe–K data for clarity.

external mass transfer limitation. This can be answered through comparison of the relative magnitudes of N_{CH_4} for the iron and the nickel catalysts. In the same range of space velocities the rate for Fe-1 ranges between 40 and 75% of that for Ni-1, yet as stated above N_{CH_4} for the latter was independent of conversion or space velocity. Thus we feel the reaction is not diffusionally limited, but the change in N_{CH_4} with conversion is the result of product inhibition, most probably by water. For iron, water inhibition has been reported in old literature (*3*), while Ni and Co do not appear to be inhibited. Varying degrees of inhibition are shown for all the other catalysts investigated here; for comparison Fe–K is also shown in Fig. 2; Fe–Co is given in Fig. 3 and Fe–Cu in Fig. 4.

It could be argued that competition would be a better term than inhibition to describe the effect of water. In this view, water would compete for active surface with adsorbed CO and lower its surface concentration by reaction to CO_2. In this way, one could actually increase the consumption of CO while decreasing that of CH_4. In light of data available for the chemisorption of water on these metals we do not believe this to be the case; however, further discussion is given subsequently.

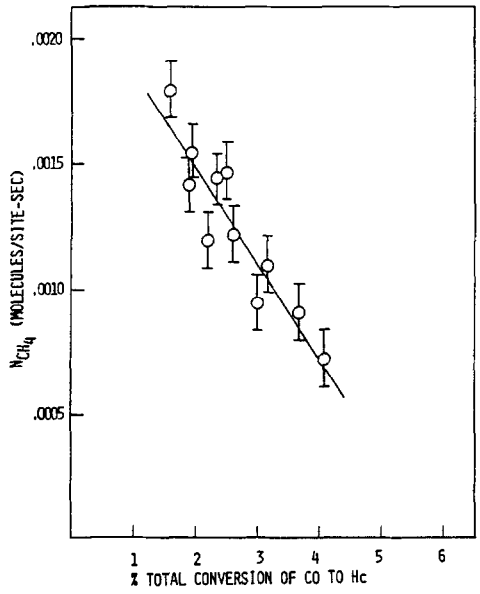

FIG. 3. Conversion dependence of N_{CH_4} for Fe–Co-1.

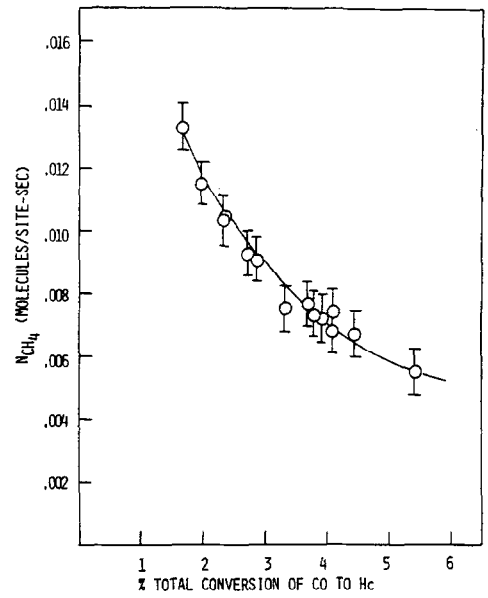

FIG. 4. Conversion dependence of N_{CH_4} for Fe–Cu-1.

2.2 Conversion dependence of the CO_2/H_2O ratio. The mole fraction of CO_2 in the reactor effluent was measured directly by gas chromatography. Water was not measured directly, but the rate of water formation was calculated by assuming that the product distribution terminated at C_5. For every mole of carbon consumed in the formation of hydrocarbons, 1 mole of water is formed; however, 1 mole of water may later be shifted to 1 mole of CO_2. Hence, at steady state, the molar rate of consumption of CO that forms hydrocarbons equals the sum of the molar rates of formation of water and CO_2. The CO_2/H_2O ratio is taken as a measure of the water–gas shift activity, with a higher CO_2/H_2O ratio at a given total conversion indicating a higher shift activity. The conversion dependence of the CO_2/H_2O ratio for catalysts Fe-1 and Fe-2 is similar and is presented in Fig. 5. A curve through the data intersects the origin,

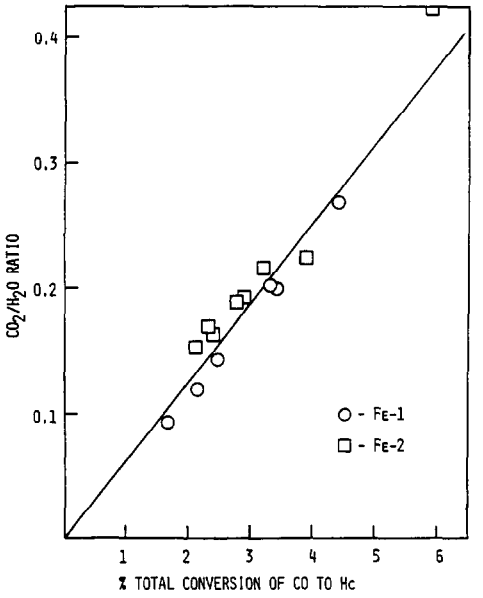

FIG. 5. Conversion dependence of the CO_2/H_2O ratio for Fe-1 and Fe-2.

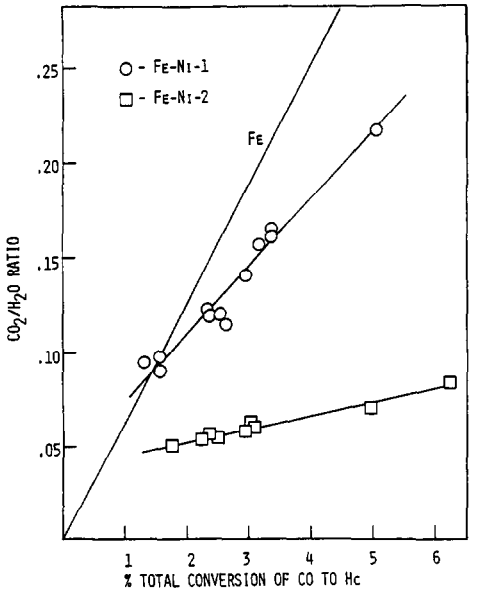

FIG. 6. Conversion dependence of the CO_2/H_2O ratio for Fe–Ni-1 and Fe–Ni-2.

confirming that water is the initial oxygen-containing product.

Catalyst Ni-1 exhibits a negligible CO_2/H_2O ratio over the conversion range of 1–6%, while Co-1 has a low but measurable ratio, increasing from 0.018 as conversion increases from 2 to 5%. These data cannot be extrapolated through the origin, but this is probably the result of analytical errors associated with measuring the small CO_2 peaks on the sloping baseline of the chromatogram.

The conversion dependence of the CO_2/H_2O ratio for the alloy and promoted catalysts is shown in Figs. 6–8. Catalyst Fe–Co-1 shows the highest shift activity, even though the shift activity of catalyst Co-1 is very small. Hence, alloying cobalt with iron is synergistic. This is attributed to the inhibition of iron carbide formation when these metals are alloyed. The iron–nickel alloys are not as interesting, since their shift activity lies between those for pure iron and pure nickel.

Catalyst Fe–K-1 is essentially catalyst Fe-1 which has been impregnated sequentially with a K_2CO_3 solution. Catalyst Fe–K-2 has the same Fe: K ratio but was prepared by simultaneous impregnation. Figure 8 indicates that simultaneous impregnation is preferred, although both promoted catalysts show a higher shift activity

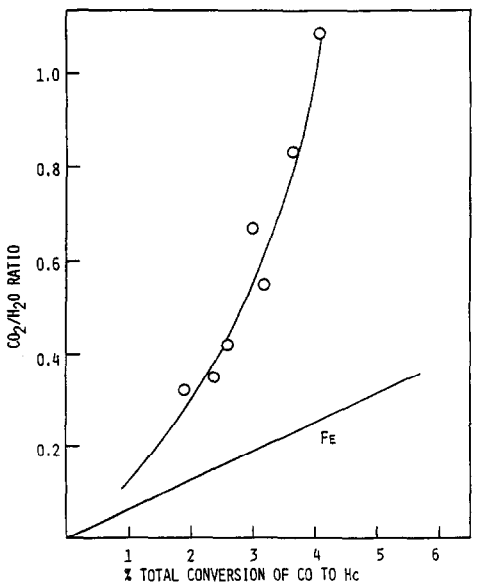

FIG. 7. Conversion dependence of the CO_2/H_2O ratio for Fe–Co-1.

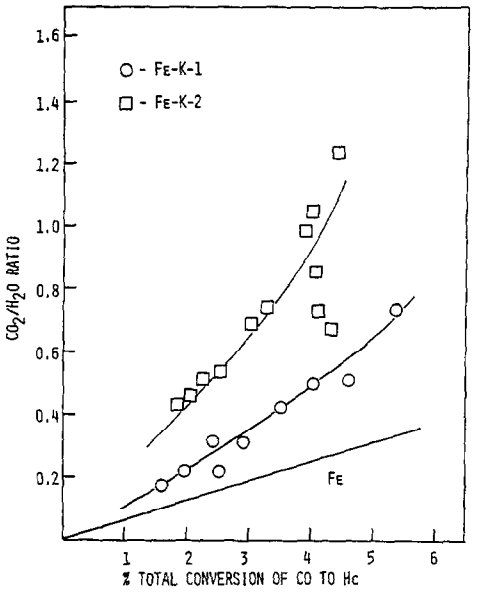

FIG. 8. Conversion dependence of the CO_2/H_2O ratio for Fe–K-1 and Fe–K-2.

than Fe-1 and Fe-2. In a separate experiment, a bed of K_2CO_3-impregnated silica was placed after Ni-1. CO_2 could not be detected; hence, potassium by itself does not possess shift activity. Catalyst Fe–Cu-1, not shown in the figures, showed the same trend but about 10% lower shift activity than Fe-1 and Fe-2, even though $Cu/ZnO/Al_2O_3$ formulations are known to possess excellent shift activity.

Since there was no evidence of long-term deactivation via carbon buildup on any of the catalysts investigated here, it is felt that any contribution to measured CO_2 from the Boudouard reaction is negligible.

2.3. Discussion of the conversion dependence of the activity and CO_2/H_2O ratio. The catalysts are rated in decreasing order of their shift activity in Table 3. The conversion dependence of N_{CH_4} is also noted; it is seen that those catalysts which do not exhibit high shift activity are not inhibited by product formation. In this regard, consider the adsorption of water vapor on single crystals of iron, cobalt, and nickel. Dwyer *et al.* (*20*) report an initial sticking coefficient of 0.56 ± 0.03 for water adsorption on Fe(001) at 200°C. Chemisorption occurs via a mobile precursor forming an immobile surface oxide or hydroxide layer. About 80% of the sites are filled at saturation. On the other hand, Tompkins (*21*) reports very little adsorption of water on the nickel surface in the absence of an electron beam. Moyes and Roberts (*22*) observed that oxidation of cobalt by water vapor is limited to the formation of a hydroxylated surface, estimated to be about half a monolayer at 295 K. This surface is passive to further water interaction, whereas cobalt reacts with oxygen to yield an oxide surface some five "layers" thick.

TABLE 3

Rating the Catalysts in the Order of Their Water–Gas Shift Activity

Catalyst[a]	Conversion dependence of N_{CH_4}
Fe–Co-1	Decreasing
Fe–K-2	Decreasing
Fe–K-1	Decreasing
Fe-1	Decreasing
Fe-2	Decreasing
Fe–Cu-1	Decreasing
Fe–Ni-1	Constant
Fe–Ni-2	Constant
Co-1	Constant
Ni-1	Constant

[a] Catalysts are listed in order of decreasing shift activity.

The low shift activity of cobalt and nickel may thus be due to their inability to chemisorb water strongly. In contrast, iron strongly chemisorbs water and exhibits high shift activity. Water competes for sites that could chemisorb CO and hydrocarbon fragments, producing the water inhibition of hydrocarbon formation on iron. No inhibition exists for the catalysts which do not strongly chemisorb water.

2.4 The relative importance of olefin hydrogenation and incorporation into growing chains. A measure of chain growth is the conversion dependence of the olefin/paraffin ratio. To determine the relative importance of olefin hydrogenation and

olefin incorporation, this ratio is compared here to the conversion sensitivity of N_{TOT}/N_{CH_4} for three catalysts: (1) Fe–Co-1 which exhibits the highest olefin/paraffin ratio; (2) Fe–K-2 which shows the highest tendency to form high-molecular-weight hydrocarbons and is an efficient olefin maker; and (3) Ni-1 which exhibits the lowest olefin/paraffin ratio. In this comparison N_{TOT} is the turnover frequency for CO consumed in forming hydrocarbons up to C_5, excluding CO_2 formation.

The conversion dependence of the steady-state $C_2^=/C_2$ ratio (open symbols) for catalysts Fe-1 and Fe-2 is presented in Fig. 9. The general trend shown for the steady-state olefin/paraffin ratio is the same for all the catalysts, decreasing with increasing conversion, consistent with the view that the initial products are olefins. The same type of behavior is observed for the $C_3^=/C_3$ ratio, although for a given conversion, the fraction of C_3 olefins is greater. Figure 9 also includes data recorded 6 min after the start of the reaction, at which point Fe-1 and Fe-2 are incompletely carburized. Isothermal carburization rates determined gravimetrically confirm this (*10, 16, 17*). The data indicate the incompletely carburized catalysts possess a lower hydrogenation potential (higher olefin/paraffin ratio). Dwyer and Somorjai (*23*) report a product that contains almost exclusively olefins over an iron single crystal and, while they do not report the exact conversion, one wonders to what extent the product distribution represents supported iron, since the crystal was surely incompletely carburized.

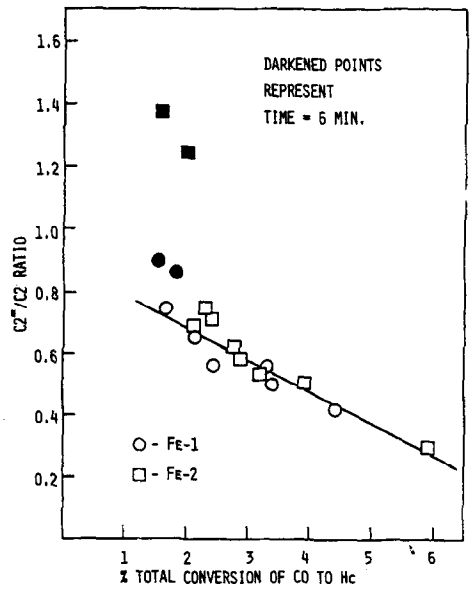

FIG. 9. Conversion dependence of the $C_2^=/C_2$ ratio for Fe-1 and Fe-2.

The chemisorptive properties of the metal and carbide may give insight into the reason for the lower hydrogenation activity of the incompletely carburized catalysts. Podgurski *et al.* (*24*) observed that a carburized iron catalyst chemisorbs less carbon monoxide than a reduced metallic catalyst. The chemisorption of hydrogen is not as strongly affected. Evidence will be presented later that suggests that carbon diffusion into catalyst Fe-1 and its subsequent carburization are rapid compared to the rate of hydrocarbon formation. Furthermore, carburization proceeds by nucleation which probably occurs at defects or grain boundaries. Hence, the surface may contain a higher fraction of metal for the incompletely carburized catalyst. The results of Podgurski *et al.* suggest the surface of the incompletely carburized catalyst would be covered with a higher CO/H_2 ratio than the catalyst at steady state. This would explain the higher olefin content.

The conversion dependence of the initial and steady-state olefin/paraffin ratios of the alloys is compared to that of the pure metals in Figs. 10–12 for $C_2^=/C_2$. Similar trends result when the data for $C_3^=/C_3$ are plotted. The catalysts are rated in decreasing order of their tendency to hydrogenate olefins in Table 4. The rating is essentially the same for $C_2^=/C_2$ and $C_3^=/C_3$ with the exception of the placement of Co-1 with respect to Fe-1 and Fe-2. Co-1 forms a higher fraction of the C_3 olefin than iron, but a lower fraction of the C_2 olefin. The data also indicate that the catalysts which

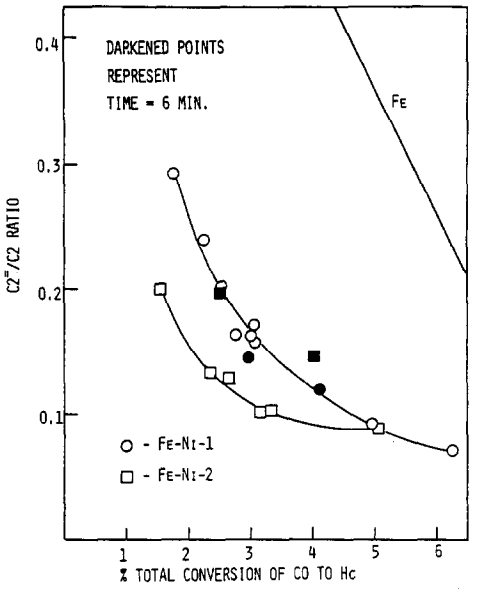

FIG. 10. Conversion dependence of the $C_2^=/C_2$ ratio for Fe–Ni-1 and Fe–Ni-2.

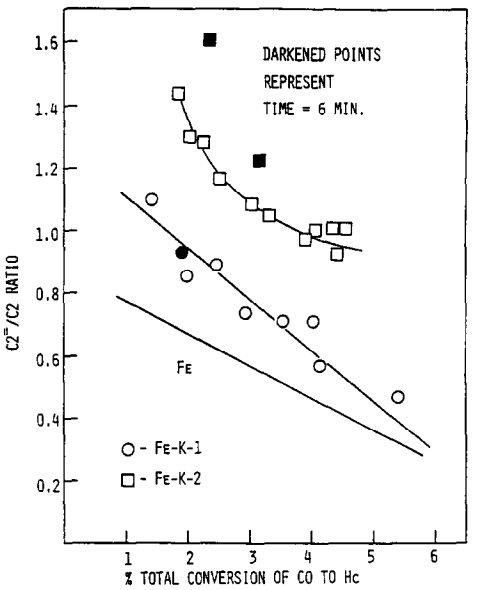

FIG. 12. Conversion dependence of the $C_2^=/C_2$ ratio for Fe–K-1 and Fe–K-2.

carburize, in general, exhibit a higher initial olefin/paraffin ratio. The catalysts which do not carburize show little time dependence of this ratio, or an initial ratio which is actually lower. Synergism is again noted in the case of catalyst Fe–Co-1 which produced the highest olefin content, even though Co-1 is only comparable to the iron catalysts. The Fe–Ni catalysts again lie between pure iron and pure nickel, while Fe–Cu-1, not shown, is very similar to Fe-1 and Fe-2.

To determine the importance of olefin in-

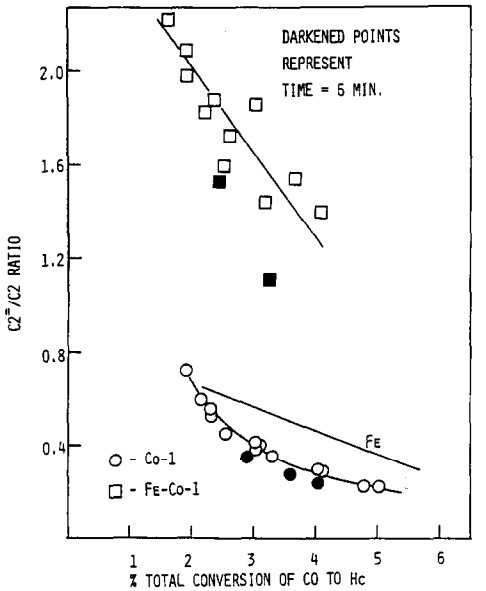

FIG. 11. Conversion dependence of the $C_2^=/C_2$ ratio for Co-1 and Fe–Co-1.

TABLE 4

Rating the Catalysts in Order of Their Tendency to Hydrogenate Olefins

For C_2[a]	For C_3[a]
Ni-1	Ni-1
Fe–Ni-2	Fe–Ni-2
Fe–Ni-1	Fe–Ni-1
Fe–Cu-1	Fe–Cu-1
Co-1	Fe-1
Fe-1	Fe-2
Fe-2	Co-1
Fe–K-1	Fe–K-1
Fe–K-2	Fe–K-2
Fe–Co-1	Fe–Co-1

[a] Listed in order of decreasing tendency to hydrogenate and increasing olefin/paraffin ratio.

corporation in controlling the selectivity to higher hydrocarbons, the conversion dependence of N_{TOT}/N_{CH_4} is plotted in Fig. 13 for catalysts Fe–K-2, Fe–Co-1, and Ni-1. Even though catalyst Fe–K-2 has the highest intrinsic ability to form hydrocarbons, its ability to incorporate initial products into growing chains is not as great as that of catalyst Fe–Co-1. Fe–Co-1 shows a 34% increase in N_{TOT}/N_{CH_4} over the range 1.5–4.5% total conversion, while catalyst Fe–K-2 shows only a 12% increase over this range. This is presumably due to the lower tendency of Fe–Co-1 to hydrogenate olefins to less reactive alkanes. Nickel has very high hydrogenation activity, so it is a poor olefin maker. N_{TOT}/N_{CH_4} increases only slightly with conversion for Ni-1. Figure 13 indicates that catalyst Fe–Co-1 may overtake Fe–K-2 in ability to produce higher hydrocarbons at higher conversion. However, caution must be exercised in making this statement, since N_{TOT} reflects only hydrocarbons up to C_5, and catalyst Fe–K-2 must certainly produce a significant fraction of C_5^+ material.

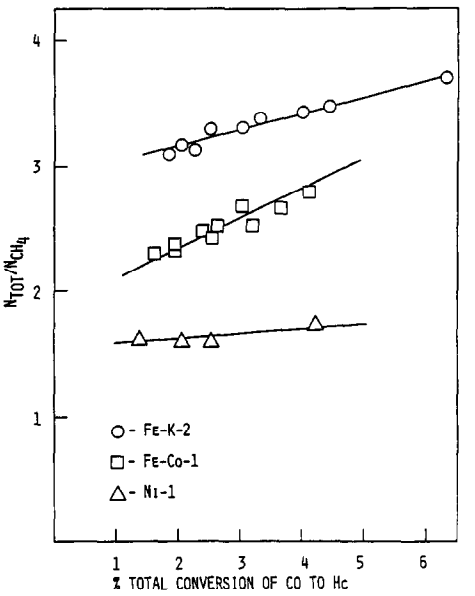

FIG. 13. Conversion dependence of N_{TOT}/N_{CH_4} for Fe–K-2, Fe–Co-1, and Ni-1.

Dry *et al.* (*6*) credit electron donation from potassium to iron for the high intrinsic ability of potassium-promoted iron catalysts to form higher hydrocarbons. Fe–K-2 forms a carbide in which Fe–C bonds are covalent and highly directional, but one may think of carbon as tending to fill the *d* band in iron. The iron–cobalt catalyst does not carburize, so the electronic structure of iron in the alloy resembles that of the pure metal. The success of Fe–Co-1 lies in the production of a catalyst with limited hydrogenation activity. Although potassium-promoted iron catalysts have a high intrinsic ability to form higher hydrocarbons, potassium also decreases the hydrogenation activ-

TABLE 5

Steady-State Product Distributions

Catalyst	Percentage total conversion	Mole percent of hydrocarbons						
		C_1	C_2	$C_2^=$	C_3	$C_3^=$	C_4	C_5
Fe–K-2	2.3 ± 0.3	58.3 ± 0.8	6.1 ± 0.2	7.6 ± 0.2	2.1 ± 0.1	12.0 ± 0.1	8.4 ± 0.3	5.2 ± 0.6
Fe–K-1	2.6 ± 0.2	62.5 ± 0.2	7.3 ± 0.4	5.9 ± 0.4	2.5 ± 0.6	11.8 ± 0.2	6.4 ± 0.4	3.6 ± 0.8
Fe-2	3.3 ± 0.1	63.1 ± 0.5	8.0 ± 0.3	5.1 ± 0.2	3.1 ± 0.2	10.4 ± 0.3	6.8 ± 0.3	3.6 ± 0.7
Fe-1	3.3 ± 0.1	63.5 ± 0.5	8.2 ± 0.2	4.6 ± 0.1	3.0 ± 0.1	10.6 ± 0.2	6.4 ± 0.2	3.7 ± 0.5
Fe–Co-1	2.0 ± 0.1	67.5 ± 0.4	4.3 ± 0.2	7.7 ± 0.3	1.2 ± 0.1	10.5 ± 0.4	5.7 ± 0.2	3.1 ± 0.1
Fe–Cu-1	3.8 ± 0.1	67.5 ± 0.3	8.6 ± 0.1	2.9 ± 0.1	3.8 ± 0.1	8.8 ± 0.2	5.9 ± 0.1	2.5 ± 0.1
Fe–Ni-2	3.0 ± 0.1	77.5 ± 0.5	8.9 ± 0.2	1.5 ± 0.1	2.4 ± 0.7	5.5 ± 0.3	3.0 ± 0.2	1.2 ± 0.3
Co-1	3.1 ± 0.1	79.3 ± 0.3	4.7 ± 0.1	1.8 ± 0.1	1.5 ± 0.2	7.1 ± 0.1	3.9 ± 0.3	1.8 ± 0.4
Ni-1	2.3 ± 0.2	82.8 ± 0.7	6.9 ± 0.2	Trace	4.3 ± 0.3	2.5 ± 0.2	2.6 ± 0.1	1.1 ± 0.1
Fe–Ni-1	2.3 ± 0.1	84.3 ± 0.5	7.1 ± 0.1	1.1 ± 0.2	2.0 ± 0.1	3.4 ± 0.3	1.7 ± 0.2	0.11 ± 0.02

ity of iron. The latter effect may ultimately be more important in determining the hydrocarbon distribution at high conversion.

2.5. Steady-state product distribution. The steady-state product distributions of the catalysts at 250°C are presented in Table 5. They are listed in decreasing order of ability to form higher hydrocarbons (assumed to be represented by the mole fraction of methane). These data represent at least five replicate analyses within the indicated range of conversion. The error assigned to these measurements represents the standard deviation.

2.6. Activity transients: clues regarding the rate-controlling step. The activity transients of Fe-1, Fe–K-1, Fe–K-2, and Fe–Cu-1 are all very similar. The transient activity of supported Fe has been correlated with the rate of carburization in previous publications (*19, 25*). For Fe-1, it has been shown (*25*) that the activity increased until carburization was complete. The following sequence is postulated to explain this phenomenon:

$$CO + H_2 \rightarrow C_s + H_2O \qquad (I)$$

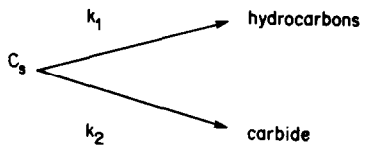

(II)

For the iron catalysts, k_2 is evidently greater than k_1 and the surface carbon forms carbide preferentially initially. After carburization only the pathway forming hydrocarbons remains and the activity reaches a steady state.

Do both paths exist for Ni-1 and Co-1? Unmuth *et al.* (*16, 17*) observed that these catalysts carburize in pure CO, which suggests that they do, so we conclude that these catalysts do not carburize in the CO/H_2 mixture because the rate of hydrocarbon formation is much greater than the rate of carbide formation. It was also noted that Fe-1 carburized faster in a 3 H_2: 1 CO atmosphere than in pure CO (*16, 17*). This indicates that the rate of carbide formation is not limited by diffusion of carbon into the bulk, but rather, by a surface reaction. There are only two ways that hydrogen could assist carbide formation: (i) the rate-controlling step involves the removal of oxygen by hydrogen following CO decomposition or, (ii) it involves hydrogen attacking a CO molecule, thus forming an oxygen-containing intermediate. An oxygen-containing intermediate seems an unlikely precursor for carbide formation, so it seems likely that oxygen removal is the rate-limiting step for the carburization of iron catalysts in pure CO.

Comparison of the initial rate of CO consumption to the steady state can provide some insight as to the rate-limiting process for hydrocarbon formation. It is postulated that the same surface carbon intermediate is involved in forming carbide and hydrocarbons. Thus, if the initial rate of CO consumption is higher, hydrogenation of the surface carbon must be slower than its rate of formation. If the initial and steady-state rates are equal, they must be limited by the same process. Since a direct analysis for water was not obtained, the absolute rates of CO consumption could not be calculated. However, one may obtain the relative rates of initial and steady-state CO consumption by comparing the areas of the H_2O and CO_2 peaks for data obtained at the same velocity. Examples of this for several catalysts are provided in Table 6. Water was clearly the major oxygen-containing product, and its rate of formation drops by less than 10%. Thus, one concludes that the rates of carbide formation and hydrocarbon formation are limited by the same process.

For carburization in pure CO, oxygen removal is rate limiting. When H_2 is present, this may not be the case. Dwyer and Somorjai (*23*) observed that after reaction over an iron crystal and subsequent pumping, no oxygen is observed on the surface by Auger spectroscopy. This suggests that oxygen removal is rapid in the presence of

TABLE 6

Initial and Steady-State Detector Response to the Oxygen-Containing Products

Catalyst	Integrator counts for CO_2			Integrator counts for H_2O		
	6 min	Steady state	Deviation	6 min	Steady state	Deviation
Fe-1	6410	6636	+3.5%	82,967	80,590	−2.9%
Fe–K-1	7827	7353	−6.1%	65,350	59,066	−9.6%
Fe–K-2	20,320	17,170	−15.5%	90,167	90,085	−0.9%
Fe–Cu-1	3701	2928	−20.9%	65,230	69,622	+6.7%

hydrogen, and hence the rate is controlled by another step. Hydrogenation of the surface carbon is ruled out as the rate-limiting step for hydrocarbon formation, since this step must also control carburization. One must conclude that C–O bond breaking controls both of these reactions.

2.7. Rating the steady-state activity. The catalysts are rated arbitrarily in the order of their activity at 1.5% conversion, and their activity over the range of conversion of 1.5–4% will be presented. The activity of the catalysts which do not exhibit product inhibition will be presented with the standard deviation of the measurements. This rating, for methanation activity, is provided in Table 7. A comparison between the rate data for the pure metals and data reported by Vannice (*15*) is also provided in Table 7. Those data were reported at 275°C, and have been corrected to 250°C using the activation energy reported. Conversion was not reported for the iron catalyst. There is fair agreement considering the difference in chemisorption techniques.

Perhaps a more meaningful comparison is provided by considering the activity for CO consumption to form hydrocarbons up to C_5. This rating is provided in Table 8. The data indicate that copper does act as a promoter for the synthesis, although it is not understood why it should. Although catalyst Fe–Co-1 was found to be very selective, Tables 7 and 8 indicate it is the least active, an order of magnitude less active than Co-1, and about a factor of 4.3 less

TABLE 7

Rating the Catalysts in Order of Their Steady-State Methanation Activity

Catalyst	N_{CH_4} (molecules/site-sec)	N_{CH_4} after Vannice (*15*) (molecules/site-sec)
Co-1	0.020 ± 0.002	0.0557
Fe–Cu-1	0.014 → 0.007[a]	
Fe–Ni-2	0.009 ± 0.001	
Ni-1	0.0075 ± 0.0004	0.0105
Fe-1	0.0065 → 0.004[a]	0.0163
Fe-2	0.0065 → 0.004[a]	
Fe–K-1	0.0055 → 0.0035[a]	
Fe–K-2	0.0055 → 0.0035[a]	
Fe–Ni-1	0.0033 ± 0.002	
Fe–Co-1	0.0016 → 0.0007[a]	

[a] From 1.5 to 4% conversion of CO to hydrocarbons up to C_5.

TABLE 8

Rating the Catalysts in Order of Their Rate of Consumption of CO Forming Hydrocarbons

Catalyst	N_{TOT} (molecules/site-sec)
Co-1	0.036 ± 0.0025
Fe–Cu-1	0.028 ± 0.016
Fe-2	0.017 → 0.012[a]
Fe-1	0.015 → 0.011[a]
Fe–K-2	0.016 → 0.012[a]
Fe–K-1	0.015 → 0.011[a]
Fe–Ni-2	0.017 ± 0.0015
Ni-1	0.012 ± 0.0005
Fe–Ni-1	0.005 ± 0.0005
Fe–Co-1	0.004 → 0.002[a]

[a] From 1.5 to 4% conversion of CO to hydrocarbons up to C_5.

TABLE 9

Activation Energies

Catalyst	E_{CH_4}[a] (kcal/mole)	E_{TOT}[a] (kcal/mole)	E_{CH_4} after Vannice (*15*) (kcal/mole)	E_{TOT} after Vannice (*15*) (kcal/mole)
Fe-1	31.3 ± 1.2	28.7 ± 3.2	18.3	28.2
Fe-2	31.1 ± 2.4	27.6 ± 3.1		
Ni-1	30.2 ± 1.9	26.4 ± 4.1	27.7	26.5
Co-1	35.6 ± 0.3	31.2 ± 1.4	31.8	22.8
Fe–Ni-1	30.7 ± 1.9	29.2 ± 5.8		
Fe–Ni-2	32.2 ± 2.3	29.5 ± 2.6		
Fe–Co-1	29.4 ± 2.4	27.9 ± 0.9		
Fe–K-1	30.3 ± 3.7	27.4 ± 4.4		
Fe–K-2	30.6 ± 2.4	27.1 ± 1.9		
Fe–Cu-1	34.1 ± 1.4	31.1 ± 5.4		

[a] Error represents 90% confidence interval from regression analysis.

active than pure iron. A true comparison would need to consider all the hydrocarbons since some of these catalysts must form a substantial amount of C_5^+ material. If the entire product distribution were obtained, the Fe–K catalysts would probably rate higher in activity than the pure Fe ones.

2.8. Activation energies. Determination of the activation energy is also affected by the problem of product inhibition, since rates must be obtained at comparable conversions. Possible conversion effects may be reflected in literature values for the activation energy on iron which varies from 15 to 25 kcal/mole (*26*). Values obtained in this work are given in Table 9 for conversions of 3.0–3.5%, in comparison with the results of Vannice (*15*).

CONCLUDING REMARKS

Electronic promotion of iron may be effective in increasing the intrinsic activity for formation of higher-molecular-weight hydrocarbon products; however, limiting the hydrogenation activity seems an equally important factor via allowing the primary olefin products to be incorporated into the growing chain. Both of these factors are seen here, particularly in a comparison of Fe–K and Fe–Co. The suppression of carbide formation also appears to play an important role. Again, cobalt is one such metal, and alloying resulted in high selectivity to olefins, high shift activity, and a high ability to incorporate olefins into growing chains.

ACKNOWLEDGMENTS

The authors are indebted to support from the Department of Energy, Office of Basic Energy Sciences, Contract DE-AC02-78ERO4993 and to the Northwestern University Materials Research Center, supported by the National Science Foundation, Materials Research Laboratories, Contract DMR76-80847, in whose Central Facilities the Mössbauer studies were performed. The comments of Professor W. N. Delgass were most helpful.

REFERENCES

1. Anderson, R. B., *in* "Catalysis" (P. H. Emmett, Ed.), Vol. 4. Reinhold, New York, 1956.
2. Pichler, H., Schulz, H., and Elstner, M., *Brennst. Chem.* **48,** 78 (1967).
3. Pichler, H., and Schulz, H., *Chem. Ing. Tech.* **42,** 1162 (1970).
4. Hall, W. K., Kokes, R. J., and Emmett, P. H., *J. Amer. Chem. Soc.* **82,** 1027 (1960).
5. Friedel, R. A., and Anderson, R. B., *J. Amer. Chem. Soc.* **72,** 1212, 2307 (1950).
6. Dry, M., Shingles, T., Boshoff, L., and Vosthuisen, A., *J. Catal.* **15,** 190 (1969).
7. Vannice, M. A., and Garten, R. L., Paper 17e,

67th AIChE Meeting, Washington, D.C., December 1974.
8. Goldschmidt, H. J., "Interstitial Alloys." Plenum, New York, 1967.
9. Amelse, J. A., Ph.D. dissertation, Chemical Engineering Department, Northwestern University, 1980.
10. Arcuri, K., M. S. thesis, Chemical Engineering Department, Northwestern University, 1979.
11. McIlwrick, C., and Phillips, C., *J. Phys. E* **6,** 1208 (1973).
12. Freel, J., *J. Catal.* **25,** 139 (1972).
13. Sashital, S. R., Cohen, J. B., Burwell, R. L., Jr., and Butt, J. B., *J. Catal.* **50,** 479 (1977).
14. Emmett, P. H., and Harkness, R. W., *J. Amer. Chem. Soc.* **57,** 1631 (1935).
15. Vannice, M. A., *J. Catal.* **50,** 228 (1977).
16. Unmuth, E., Ph.D. dissertation, Chemical Engineering Department, Northwestern University, 1979.
17. Unmuth, E., Schwartz, L. H., and Butt, J. B., *J. Catal.* **63,** 404 (1980).
18. Romig, A. D., and Goldstein, J. I., *Metall. Trans. A* **92,** 1599 (1978).
19. Raupp, G. B., and Delgass, W. N., *J. Catal.* **58,** 337 (1979).
20. Dwyer, D. J., Simmons, G. W., and Wei, R. D., *Surf. Sci.* **64,** 617 (1977).
21. Tompkins, H. G., *Surf. Sci.* **62,** 293 (1977).
22. Moyes, R. B., and Roberts, M. W., *J. Catal.* **49,** 216 (1977).
23. Dwyer, D. J., and Somorjai, G. A., *J. Catal.* **56** 249 (1979).
24. Podgurski, H. H., Kummer, J., Dewitt, T., and Emmett, P. H., *J. Amer. Chem. Soc.* **72,** 5382 (1950).
25. Amelse, J. A., Butt, J. B., and Schwartz, L. H., *J. Phys. Chem.* **82,** 558 (2978).
26. Vannice, M. A., *J. Catal.* **37,** 462 (1975).